Central European Science Journals
w w w . c e s j . c o m

Central European Journal of Physics
Central European Science Journals
CEJP 2(1) 2004 147–159

Fowler-Nordheim tunnelling in Au-TiO_2-Ag film structures

J. Aarik[1] *, V. Bichevin[1], I. Jõgi[2], H. Käämbre[1], M. Laan[2†] V. Sammelselg[1]

[1] *University of Tartu, Institute of Physics, Riia 142, 51014 Tartu, Estonia*

[2] *University of Tartu, Institute of Experimental Physics and Technology, Tähe 4, 51010 Tartu, Estonia*

Received 18 June 2003; accepted 10 October 2003

Abstract: I-V-characteristics have been measured for Au-TiO_2-Ag structures with TiO_2 layers of 30 and 180 nm thickness. The TiO_2 films were grown by atomic layer deposition (ALD) technique. In the case of negative bias on the Au electrode, the conduction currents through TiO_2 layers follow the Fowler-Nordheim formula for field emission over several orders of magnitude. The bulk of the currents may be attributed to tunnelling, seemingly through a Schottky barrier at the Au-TiO_2 junction. In the case of reversed polarity the currents are also observed, but cannot be interpreted as tunnelling.

Keywords: titanium dioxide, thin films, electrical properties, Fowler-Nordheim plots, tunnelling currents
PACS (2000): 73.40.Gk, 73.40.Rw

1 Introduction

Titanium dioxide has several applications. Attempts have been made to use it in conductometric gas (e.g. oxygen) sensors [1] and as a high-k gate insulator [2]. Very recently it was included into a novel merbromin/Au/TiO_2/Ti photovoltaic device (solar cell) [3]. Some of us have shown [4] that a TiO_2film, covering a point electrode in a negative corona gap, facilitates the occurrence of the discharge. Vu Thien Binh and associates have re-

* E-mail: henn@fi.tartu.ee
† E-mail: laan@ut.ee

cently developed an efficient planar cold cathode, based on TiO_2 ultrathin film coatings on metal substrates [5], [6]. These cathodes are far more technological, and run nicely in a lower vacuum and at lower voltages than the conventional ones.

In the present paper we report some peculiarities of the current-voltage dependence of metal-oxide-metal (MOM) structures, containing TiO_2 films.

2 Experimental

2.1 Preparation of samples

The MOM structures were prepared on Si(1 0 0) substrates and consisted of an Au electrode, a TiO_2 layer, and an Ag counter electrode. Before formation of the structure, the substrates were etched in HF and rinsed in de-ionized water. Then the Au-electrode was deposited by vacuum evaporation. A typical thickness of this electrode was around 300 nm.

Titanium dioxide films were grown using atomic layer deposition (ALD), a cyclic process consisting of a periodically repeated series of self-limited surface reactions (for more information, see, e.g. [7], [8] and literature therein). The deposition was performed in a low-pressure flow-type reactor using $TiCl_4$ as the titanium precursor and H_2O vapour as the oxygen precursor. To synthesise a film, the substrates were alternately exposed to the titanium and oxygen precursors, which were carried to the substrates in a flow of nitrogen gas. Between each exposure, the reactor was purged with pure N_2. Thus, the process consisted of cycles, which contained exposures to metal and oxygen precursors and following purge periods. The thickness increment per cycle ranged from 0.053–0.078 nm in the case of substrate temperatures (225–275 ^{o}C) and precursors used in this work. We applied 500 and 2300 cycles to grow films from $TiCl_4$ and H_2O. The thicknesses obtained were 30 and 180 nm, respectively.

2.2 The structure of the samples

To have some concept of the structure and surface morphology of the TiO_2 films, we studied reference samples grown on bare Si(1 0 0) substrates in the same processes as the films for conductance measurements. Reflection high-energy electron diffraction and X-ray diffraction studies revealed anatase phase in all these films.

The surface microstructure of TiO_2 films was studied with a multimode scanning probe microscope AutoProbe CP, PSI/ThermoMicroscopes/Veeco. The microscope worked in intermittent contact atomic force mode, and the samples were exposed in air. Silicon cantilevers (Ultralevers^{TM}, PSI), having conical probes and tip radii <10 nm were used in these studies. The row images of the microscope were filtered for low frequency noise using image-processing package IP2 from PSI. The same package was used for calculating root mean square (RMS) roughness of the film surface.

The obtained images are shown in Figure 1. As can be seen, the surface roughens

drastically with increasing film thickness. The calculated RMS roughness (R) confirms this trend: it increases from 3.5 nm to 11.4 nm with the increase of the mean film thickness from 30 to 180 nm. Whereas the R of Si surface was below 1 nm, the RMS thickness variations of the films reached 10% of their total thickness. This result shows that during electrical measurements the local electric fields can be rather variable over the film surface because the curvature of different parts of the painted electrode, repeating the relief of the oxide, can be highly inhomogeneous. The AFM data also show that exchange of the titanium precursor, i.e. using $Ti(OC_2H_5)_4$ instead of $TiCl_4$, has no noticeable influence on the relative surface roughness of the TiO_2 films grown. Our R values are in accordance with these obtained earlier [7], [8] for TiO_2 films of the same thickness but they are by an order higher than R for the oxide films (HfO_2, SiO_2, ZrO_2), deposited by using a dual ion beam sputtering system, as reported in [9]. As discussed earlier [7], [8], the main reason for the significant surface roughness of TiO_2 films is evolution of microcrystals during the film growth.

2.3 Conductance measurements

The current-voltage curves were recorded in a standard circuit in the dc mode (Figure 2, inset). A counter spot electrode needed for these measurements was formed painting a silver suspension onto the TiO_2 layer. The sample was connected into the circuit using thin platinum wires that were in contact with the Ag spots on the Au film and the oxide layer.

The current was measured with a multi-range galvanometer M 193, having maximal sensitivity $4{\cdot}10^{-8}$ A per division, and voltage – by a digital voltmeter Ш 4300. The applied voltage was varied in the interval from 10^{-3} to 10 V. The currents ranged from 10^{-8} to 10^{-2} A. The experimental current densities were calculated by dividing measured current by apparent film area. The measurements were carried out at room temperature in the laboratory atmosphere. Each measurement series included a step-wise increase of the applied voltage and fixation of the mean current at each step.

3 Results and discussion

3.1 The current-voltage characteristics

The tested films had nonlinear I-V-characteristics (Figure 2). As the same Figure shows, the I-V plots turned out to be different for the differing polarity of the connection of the Au-TiO_2-Ag sandwich into the test circuit, i.e. for the cases of negative or positive bias on the Au electrode, further labelled as Au(–) or Au(+) polarity.

3.2 The Au(–) case: a Fowler-Nordheim tunnelling

There is a great variety of the thin film conductance mechanisms [10]. Attempting to approximate the I-V curves by some analytic expression, we revealed that for the Au(–) polarity, the I-V dependence can be satisfactorily fitted by the Standard Fowler-Nordheim equation, describing, in general, the field emission current from a metal into vacuum [11], [18]:

$$J = at_F^{-2}\phi^{-1}E^2 \cdot \exp\left(-\frac{bv_F\phi^{3/2}}{E}\right), \tag{1}$$

where

$$a \equiv e^3/8\pi h = 1.541 \cdot 10^{-6},$$
$$b \equiv \tfrac{4}{3}(2m)^{1/2}\Big/e\hbar = 6.831 \cdot 10^9.$$

Here, J is the current density (A/cm^2), ϕ is the emitter's work function (eV), E the applied field strength (V/m), e the elementary positive charge (C), m the electron effective mass (kg), h the Planck's constant (J·s), $\hbar = h/2\pi$, v_F and t_F are the values of the special field emission elliptic functions v and t [18], evaluated for a barrier of height ϕ.

In so-called Fowler-Nordheim coordinates, this equation takes the form:

$$\ln\left(\frac{J}{E^2}\right) = \ln\left(at_F^{-2}\phi^{-1}\right) - \frac{\left(bv_F\phi^{3/2}\right)}{E}. \tag{2}$$

An experimental Fowler-Nordheim plot is modelled by the tangent to this curve, taken in the mid-range of the experimental data. This tangent can be written in the form [11]

$$\ln\left(\frac{J}{E^2}\right) = \ln\left(ra\phi^{-1}\right) - \frac{\left(bs\phi^{3/2}\right)}{E}, \tag{3}$$

where r and s are the appropriate values of the intercept and slope correction factors, respectively.

Typically, s is of the order of unity, but r may be of order 100 or greater. Both r and s are slowly varying functions of 1/E, so a Fowler-Nordheim plot is expected to be a straight line.

The formula (1) was originally derived to describe the field emission current from metals into vacuum. However, in our case it applies for the conduction current in a MOM sandwich structure. Examining literature, one finds that quite similar cases were revealed as early as 1967-69 for a Mg-SiO_2-Si structure [12], [13] and an Al-AlN-Al structure [14].Very recently the Fowler-Nordheim tunnelling was also observed in magnetron sputtered TiO_2 layers [2].

The Fowler-Nordheim equation assumes the electron transport from metal to vacuum by tunnelling. Thus, the conductivity in a MOM structure, obeying the same law, should be also of tunnelling nature. As Snow noticed [12] already in 1967, the 10 to 10^2 nm oxide layers are much too thick for direct tunnelling through the oxide. Thus, in full accordance

with [12–15], we believe that the tunnel effect occurs through the field-thinned Schottky barrier at the Au-TiO_2 interface and manifests itself in the straight-line F-N plots. (In [2], for Si-TiO_2 systems, a tunnelling via SiO_2 interlayer is assumed. So as our TiO_2 layers are separated from the Si substrate by the gold electrode, this alternative is hardly applicable in our case.)

A simplified band diagram in Figure 5 illustrates the conduction process. Electrons, tunnel-injected into the oxide conduction band, move through the oxide and are picked up by the Ag counter-electrode (cf. [16], p. 454, Figure 10.17). The process can be characterised also as an internal field emission [16].

In our preliminary Fowler-Nordheim tests we estimated the field strength E as $E = U/d$, where U is the voltage, applied to the MOM structure, and d the oxide thickness. However, a more refined consideration ([10], p. 635) shows that in the case if a Schottky barrier (blocking contact) is involved, almost all the voltage drop occurs on the barrier and the field strength in the formulas (1) and (2) should properly be calculated according the relation

$$E = \sqrt{\frac{2N_d eU}{\varepsilon\varepsilon_o}} = 0.1902\sqrt{\frac{N_d U}{\varepsilon}} \ \frac{\mathrm{V}}{\mathrm{m}}. \tag{4}$$

Here, N_d is the concentration of donors (cm^{-3}), ε is dielectric constant of the oxide and ε_o is the electric constant.

Thus, (2) should be rewritten in the form

$$\ln\left(\frac{J}{U}\right) = \ln\left(ra'\phi^{-1}N_d\varepsilon^{-1}\right) - \frac{\left(b's\phi^{3/2}\varepsilon^{1/2}N_d^{-1/2}\right)}{\sqrt{U}}, \tag{5}$$

where

$$a' \equiv 2ae/\varepsilon_0 = 5,578 \cdot 10^{-14},$$
$$b' \equiv b\sqrt{\varepsilon_0/2e} = 3,591 \cdot 10^{13}.$$

Figures 4a and 4b demonstrate the plots of our conductance data in the coordinates of formula (5). Figure 4a shows for the Au(–) polarity a pretty fit of the experimental points onto the Fowler-Nordheim plot over many decades.

In accordance with the theory, there is a close coincidence of the F-N-plots for the samples of different thickness. Indeed, the field strength at the blocking contact should not depend on the thickness of the dielectric layer [10].

At lower E,higher $V^{-1/2}$ values, a deviation from the linear F-N plot occurs (especially pronounced is the nonlinearity for the 180 nm films, (Figure 4). Analogous nonlinearity appears in field-induced external emission from amorphous diamond films [17]. The authors have suggested that this nonlinearity originates from a transition from field emission to thermionic emission as the applied field decreases. Their numerical calculations on the basis of a unified electron emission theory [18], embracing both field and thermionic emission, are consistent with the experimental data. Plausibly, analogous considerations are valid in our case: at lower fields the Schottky barrier could be thermally overcome.

We have attempted to assess the effective work function ϕ value, from the slope of the F-N-plots according to formulas (4) and (5). The intercept was not used because the actual area of emission through which electrons tunnel was unknown. Having no reliable data about the electron effective mass m_e value in TiO_2, we assumed, as a first approximation, $m_e = m$, where m is the free electron mass. Besides, according to [11], we approximated the constant s in the formula (5) with unity. Then we need the values of ε and N_d. The authors of [2] and [5] give for $TiO_2$the values $\varepsilon = 80$ and $\varepsilon = 35$, respectively. Assuming for the estimates $\varepsilon = 50$ and $N_d = 10^{18}$ cm^{-3}, one gets $\phi = 0.17$ eV. Similar low ϕ value was calculated in the paper [6] for Pt–TiO_2 junctions (see also [16]). There the small work function ϕ as explained by space charge effects in the thin semiconductor film. Obviously, in our case the estimated ϕ value represents the height of a metal/semiconductor Schottky barrier.

3.3 The Au(+) polarity

In this case, the I-V-characteristics cannot be transformed in good F-N-plots. The linear part on the ln $(J/U) \sim U^{-1/2}$ dependence, if any, covers only a couple of decades.

The reason of the worse quality of the F-N-plots for the Au(+) case can be in the great roughness of the oxide surface (Figure 1). The emulsion-formed Ag electrode surface, being a replica of the oxide, repeats the rough surface relief. The curvature of individual Ag relief protrusion tips, determining the local E value, becomes randomly distributed. Due to this E-scatter, a distinctive linear F-N plot can be smeared. The scatter can be even enhanced by the percolative character of the conductivity *via* individual silver grains in the organic binder of the emulsion. This random walk is perceptibly manifested in the current fluctuations (noise), being by an order bigger at the Au(+) bias as compared with the Au(–) case.

4 Conclusions

In summary, Fowler-Nordheim tunnel currents have been observed in TiO_2 films, prepared by atomic layer deposition. Commonly it is thought that tunnelling field emission appears from sharp points, concentrating the field intensity. Our results demonstrate, in accordance with [12–15], that there exist favourable conditions for tunnelling process to appear also from an apparently flat metal surface into a semiconductor layer. Notice that due to their rather high leakage currents by tunnelling, the ALD-grown TiO_2 layers are not perspective candidates for high-k gate insulators in the field effect transistors.

Acknowledgements

The authors are thankful to Dr. H. Mändar and Dr. T. Uustare for structural characterisation of the TiO_2 films. Thanks are also due to Prof. Vu Thien Binh and Dr. H.Nakane

for consultations and providing their publications. The work was financially supported by the Estonian Science Foundation (grants No 5028 and 5032).

References

[1] J. Sheng, N. Yoshida, J. Karasawa and T. Fukami: "Platinum doped titania film oxygen sensor integrated with temperature compensating thermistor", *Sens. Actuators B*, Vol. 41, (1997), pp. 131–136.

[2] M. Kadoshima, M. Hiratani and al.: "Rutile-type TiO_2 thin film for high-k gate insulator", *Thin Solid Films*, Vol. 424, (2003), pp. 224–228.

[3] E.W. McFarland and J. Tang: "A photovoltaic device structure based on internal electron emission", *Nature*, Vol.421, (2003), pp. 616–618.

[4] V. Repän, M. Laan, P. Paris, J. Aarik and V. Sammelselg: "Negative coronas: low current mode - pulse mode transition", *Czech. J. of Phys.*, Vol. 49, (1999), pp. 217–224.

[5] V.T. Binh and Ch. Adessi: "New mechanism for electron emission from planar cold cathodes: the solid-state field-controlled electron emitter", *Phys. Rev. Lett.*, Vol. 85, (2000), pp. 864–867.

[6] V.T. Binh, V. Semet and J.P. Dupin: "Novel electron sources", *Electrochem. Soc. Proc.*, Vol. 2000, (2001), pp. 157–166.

[7] J. Aarik, A. Aidla, H. Mändar, T. Uustare and V. Sammelselg: "Anomalous effect of temperature on atomic layer deposition of titanium dioxide", *J. Crystal Growth*, Vol. 220, (2000), pp. 531–537.

[8] J. Aarik, A. Aidla, H. Mändar, T. Uustare and V. Sammelselg: "Influence of structure development on atomic layer deposition of TiO_2 thin films", *Appl. Surf. Sci.*, Vol. 181, (2001), pp. 339–348.

[9] M. Alvisi, G. Leo, A. Rizzo, L. Tapfer and L. Vasanelli: "Surface and interface morphology of thin oxide films investigated by X-ray reflectivity and atomic force microscopy", *Surface and Coatings Technology*, Vol. 100–101, (1998), pp. 76–79.

[10] J.G. Simmons: "Conduction in thin dielectric films", *J. Phys. D: Appl. Phys.*, Vol. 4, (1971), pp. 613–657.

[11] R.G. Forbes: "Refining the application of Fowler-Nordheim theory", *Ultramicroscopy*, Vol. 79, (1999), pp. 11–23.

[12] E.H. Snow: "Fowler-Nordheim tunneling in SiO_2 films", *Solid State Comm.*, Vol. 5, (1967), pp. 813–815.

[13] M. Lenzlinger and E.H. Snow: "Fowler-Nordheim tunneling into thermally grown SiO_2", *J. Appl. Phys.*, Vol. 40, (1969), pp. 278–283.

[14] G. Lewicki and C.A. Mead: "Currents through thin films of aluminium nitride", *J. Chem. Phys.Solids*, Vol. 29, (1968), pp. 1255–1267.

[15] V.V. Zhirnov, G.J. Wojak, W.B. Choi, J.J. Cuomo and J.J. Hren: "Wide band gap materials for field emission devices", *J. Vac. Sci.Technol. A*, Vol. 15, (1997), pp. 1733–1738.

[16] S.A. Fridrikhov and S.M. Movnin: *Physical foundations of electronics*, Vyshaya Shkola, Moscow, 1982, pp. 454, (In Russian).

[17] N.S. Xu, Jun Chen and S.Z. Deng: "Physical origin of nonlinearity in the Fowler-Nordheim plot of field-induced emission from amorphous diamond films: Thermionic emission to field emission", *Appl. Phys. Lett.*, Vol. 76, (2000), pp. 2463–2465.

[18] E.L. Murphy and R.H.Jr. Good: "Thermionic emission, field emission, and the transition region", *Phys. Rev.*, Vol. 102, (1956), pp. 1464–1473.

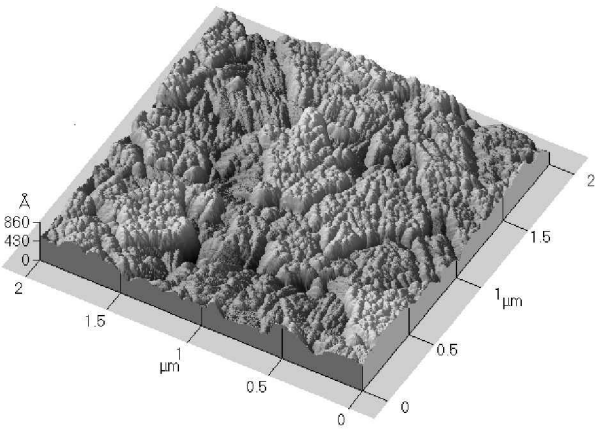

a)

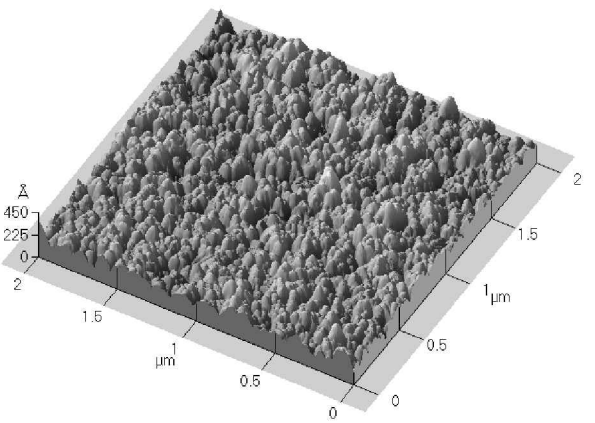

b)

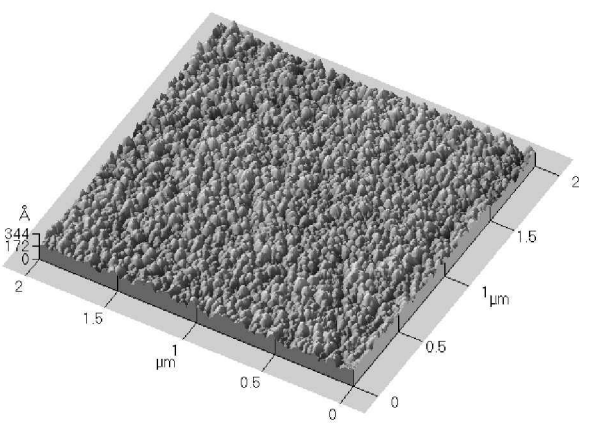

c)

Fig. 1 Surface topography of TiO_2 thin films with thicknesses of a – 180 nm, b – 80 nm, and c – 30 nm, depicted with atomic force microscope in intermittant contact mode. The RMS roughness of the film surfaces is 11.4, 5.3, and 3.5 nm, respectively.

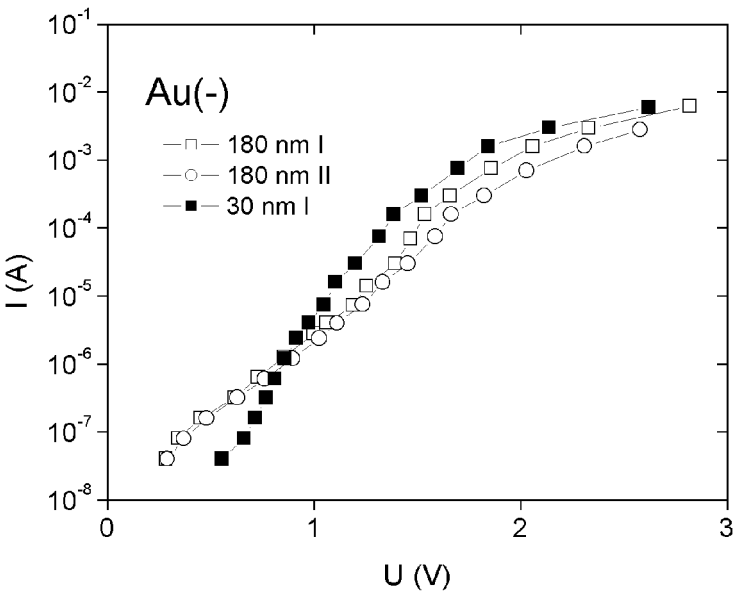

a)

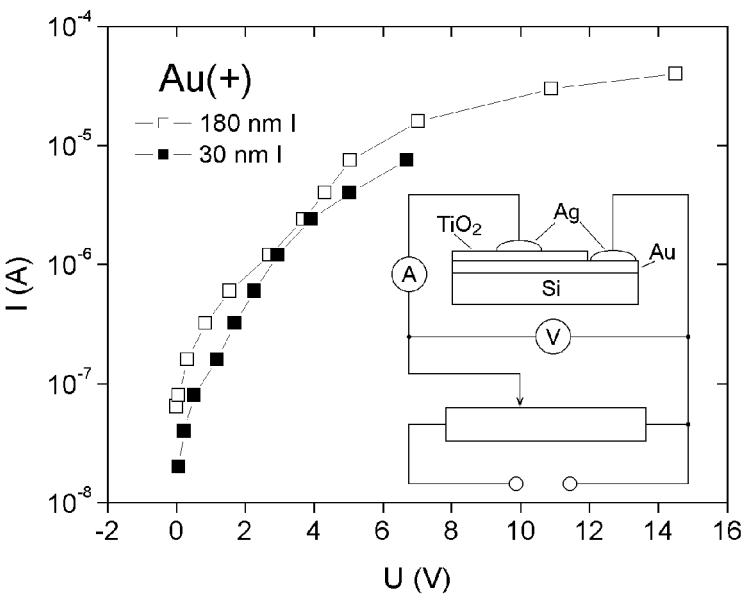

b)

Fig. 2 I-V characteristics of Au-TiO_2-Ag structures including TiO_2 layers of different thickness (indicated; I, II – different samples), for Au biased negatively, Au(–), or positively, Au(+). Inset: the measuring circuit diagram.

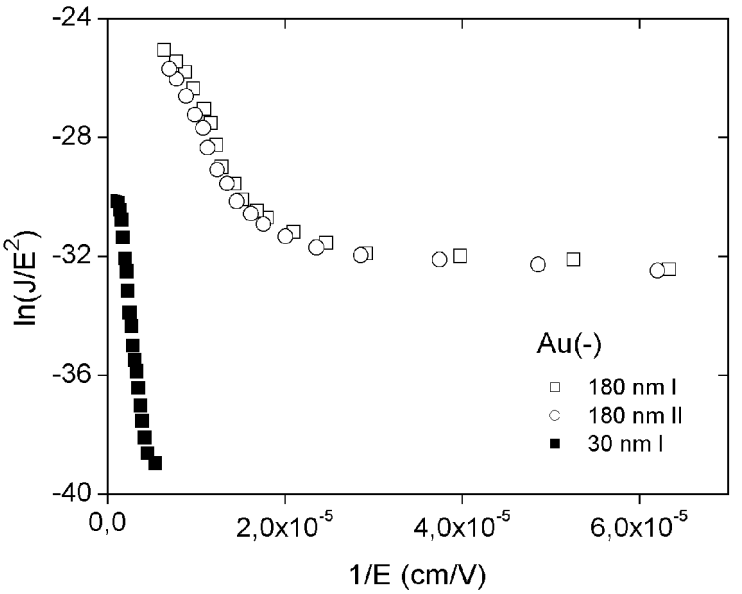

a)

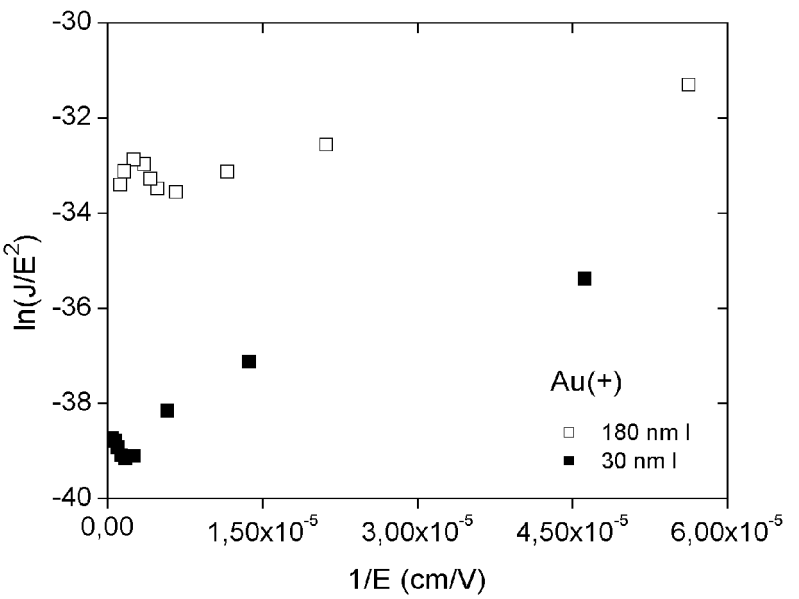

b)

Fig. 3 Plots of $\ln(J/E)$ vs E^{-1} for currents through Au-TiO_2-Ag structures including TiO_2 layers of different thickness (indicated; I, II – different samples). Au(–) – Au negatively biased, Au(+) – Au positively biased. J – in A/cm^2, E – in V/cm.

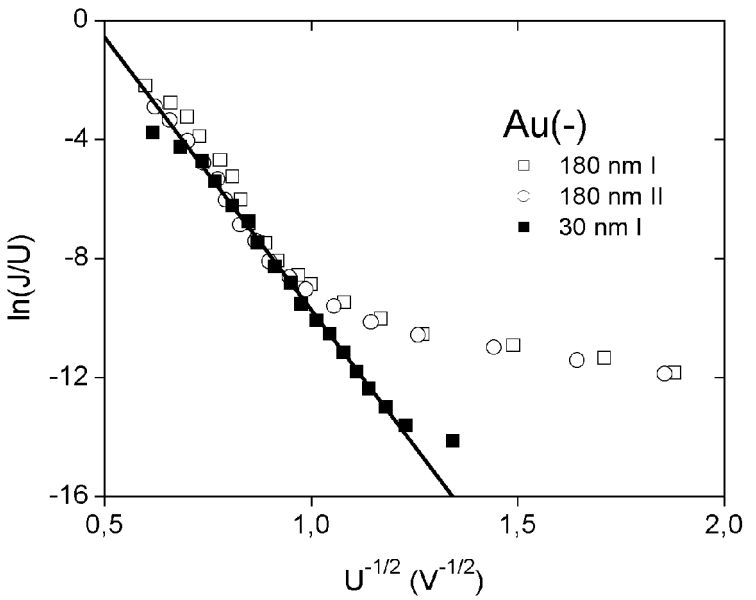

a)

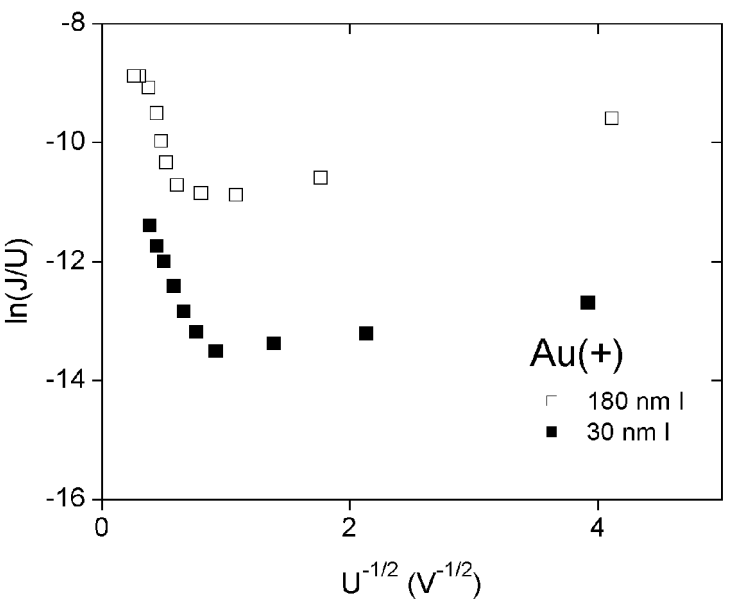

b)

Fig. 4 Plots of $\ln(J/U)$ vs $U^{-1/2}$ derived from Fowler-Nordheim equation (assuming $E \sim U^{1/2}$,see formula (4)) for currents through Au-TiO_2-Ag structures including TiO_2 layers of different thickness (indicated; I, II – different samples). Au(–) – Au negatively biased, Au(+) – Au positively biased. The straight line is a least squares fit for the 30 nm specimen. J – in A/cm^2, U – in V.

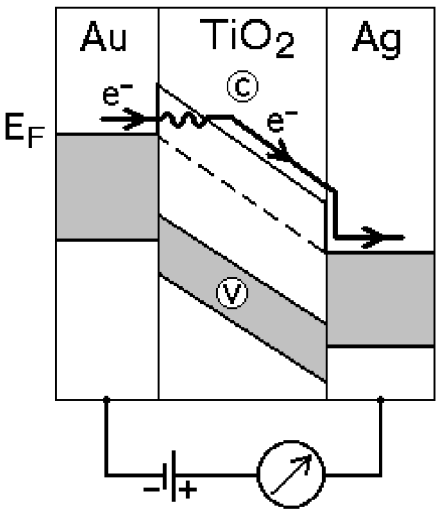

Fig. 5 Simplified band diagram of the electron (e^-) current in an Au-TiO_2-Ag structure; E_F – the Fermi level, C conductance and V valence band of TiO_2.